Title
ON THE CLIMB OF DISLOCATIONS IN BORON ION IMPLANTED SILICON

Author
Wu, Wei-Kuo

Publication Date
1977-07-01

Submitted to Journal of Applied Physics

LBL-5452
Preprint

ON THE CLIMB OF DISLOCATIONS IN BORON ION IMPLANTED SILICON

Wei-Kuo Wu and Jack Washburn

July 1977

Prepared for the U. S. Energy Research and Development Administration under Contract W-7405-ENG-48

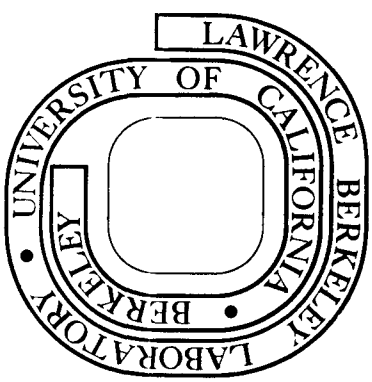

DISCLAIMER

ON THE CLIMB OF DISLOCATIONS IN BORON ION IMPLANTED SILICON

Wei-Kuo Wu and Jack Washburn

ABSTRACT

The climb of dislocations, both perfect ($\bar{b} = \frac{1}{2}\langle 100\rangle$) and imperfect ($\bar{b} = 1/3\ \langle 111\rangle$) was studied in boron implanted silicon thin foils by electron microscope observation of the shrinkage of interstitial type dislocation loops. The temperature dependence of the climb rate gave an apparent activation energy of 5.6 ± 0.5 ev for both types. The imperfect loops adopted a rounded shape during shrinkage but tended to acquire straight segments whenever the climb motion required nucleation of new jog pairs. Climb rate at a given temperature was shown to be a function of the climb force on the dislocation and on the distance to the nearest efficient sink or source. The surfaces of the foil were shown to be relatively poor sinks for interstitials or alternatively poor sources for vacancies.

I. Introduction

Dislocation climb rates can be studied conveniently by transmission electron microscopy[1-7] by measuring the shrinkage rate or migration rate of dislocation loops. The technique of repeated observation of the same area with intermediate annealing at an accurately known temperature in a furnace has made possible determination of self-diffusion coefficients and activation energies without the use of radioactive tracers.[8] It has also been possible to study pipe diffusion along dislocation cores.[6,7] Most previous observations of loop shrinkage have been made on vacancy loops obtained by quenching and aging or in the case of magnesium oxide on loops formed by break-up of dipoles during high temperature annealing of plastically deformed crystals.

In the present work, the technique is applied to interstitial loops in silicon which are formed during annealing after ion implantation of boron. Both faulted loops with burger's vector 1/3 <111> and perfect loops with burger's vector $\frac{1}{2}$ <110> are obtained.

II. Experimental

Silicon slices, 5 Ω-cm, n-type of <111> orientation were implanted at room temperature with boron ions at 100 kev to a dose of $2 \times 10^{14}/cm^2$.

A piece of $\frac{1}{2}$ in. x 1 in. was taken from the <111> slice and annealed for 20 minutes at each temperature from 400°C up to 1050°C with 50°C steps in a quartz tube furnace. A flowing dry nitrogen atmosphere was used.

Specimens for electron microscope observations of 3mm in diameter were cut from the above after the 1050°C anneal. They were then chemically polished from the unimplanted side as described previously[9].

The thin foil was then repeatedly examined in the Philips 301 trans-

mission electron microscope operating at 100 kv. Between successive observations the thin foil was furnace annealed. The annealing temperatures were monitored to an accuracy within ±1°C by a chromel-alumel thermocouple sealed in a small quartz tube positioned near the specimen.

It was observed that clean annealing could always be obtained in dry nitrogen flow not only for bulk specimens but also for thinned foils up to about 1000°C .

All micrographs were taken under two beam diffraction conditions with S>0, where S is the deviation vector away from the exact Bragg condition. Accurate repetition of diffraction conditions and orientation of the foil throughout a series was achieved by making use of the Kikuchi map[9].

III. Mechanisms of Climb of Dislocation Loops

a) Diffusion vs. Emission Controlled Mechanism

There are two extreme cases for the shrinkage of dislocation loops. Silcox and Whelan[1] proposed that the rate of shrinkage in aluminum foils was controlled by the rate of emission of vacancies at jogs. Later, Seidman and Balluffi[10] showed that the rate controlling process for aluminum could be the diffusion of vacancies away from the immediate vicinity of the loops. Theoretical considerations[11] indicate that the two possibilities lead to essentially the same functional form of the rate equation.

However, the shrinkage rate if determined by the emission of the point defects is independent of the distance between the dislocation loop and the sources or sinks for the point defects, whereas for diffusion controlled climb, this should not be the case. This difference can provide a criterion for determining whether the climb rate of a dislocation is emission or diffusion controlled in a particular case[12].

b) Vacancy vs. Interstitial Mechanism

Dislocation climb requires either the formation and migration of vacancies or the formation and migration in the opposite direction of interstitials. In the temperature range above 900°C, it is not absolutely clear which mechanism operates in silicon. In order to explain experimentally observed abnormal impurity concentration profiles[13] which were not of the expected complementary error-function type, Dobson[14,15] concluded that solute diffusion in silicon occurred by the interstitialcy mechanism. Similarly, Prussin[16] attributed the growth of stacking faults and dislocation loops during wet oxidation to the continuous generation of interstitials and destruction of vacancies at the silicon-oxide interface. Seeger[17] has also pointed out that to account for the unusually large pre-exponential factor for self-diffusion at high temperatures (>900°C) in silicon an interstitial mechanism is needed.

The temperature range in this study is between 940°C to 1000°C, therefore, a self-interstitial mechanism will be assumed for the purpose of discussion.

IV. Model for Shrinkage of Circular and Elongated Interstitial Loops

Interstitials are formed or absorbed along a dislocation line according to the sign of the climb force. Therefore, a flux of interstitials passes between near-by dislocation segments of different or opposite curvature (where the driving force for climb is unequal or in opposite directions). The foil surfaces also can act as a sink for interstitials.

The climb force per unit length for a dislocation loop of radius r can be expressed as:

$$F_c = \frac{3Gb^2}{8\pi r}\left[\ln\left(\frac{22r}{b}\right) - 0.37\right] + \gamma \qquad (1)$$

where G, b, r and γ are the shear modulus, burger's vector, radius of loop and stacking fault energy respectively.

The climb rate for both emission control and diffusion control is given for circular loops of radius r by an expression of the form:

$$\frac{dr}{dt} = -AD\left[e^{\frac{F_c B^2}{kT}} - \frac{C_1}{C_0}\right] \qquad (2)$$

where A is a constant, D is the silicon self-diffusion coefficient. $D = D_0\, e^{-u/kT}$ where u is the activation energy for self diffusion, C_1 and C_0 are the non-equilibrium and equilibrium concentrations of interstitials respectively.

For diffusion control the local equilibrium concentration of interstitials near the dislocation, determined by the value of F_c, is nearly maintained during climb and the climb rate is then determined primarily by the diffusion flux. F_c increases as r decreases.

For emission control the local concentration of interstitials near the climbing dislocation remains close to the thermal equilibrium value and climb rate is determined primarily by the rate of emission. The shrinkage rate for elongated dislocation loops of length L shrinking only along the long direction can be expressed as:

$$\frac{dL}{dt} = -A'\, D\left(e^{\frac{F_c B^2}{kT}} - \frac{C_1}{C_0}\right) \qquad (3)$$

In this case F_c is independent of L.

V. Results

a) General.

Figure 1 shows a series of pictures of the same loops after each of eight annealing treatments. The loops are all faulted with burger's vector 1/3<111>. Loops $\overline{B}$ and $\overline{C}$ lie on the {111} plane which is parallel to the foil surfaces and all others are on an inclined {111} plane. Loop F is cut by the foil surface, D is very near the surface and the others in the same line lie at increasing depths.

During the annealing between pictures 1 and 2, the foil was subjected to strongly oxidizing conditions. All loops larger than loop G grew slightly and developed <110> edges. This is consistent with the observations of Prussin[16] and suggests that oxidation increases interstitial concentration at the surfaces enough to reverse the direction of the net climb force for the larger loops. During all other annealing runs oxygen was largely excluded by the flow of dry nitrogen. All loops were observed to shrink at a rate depending on their size. The driving force for shrinkage increases with decreasing loop size because of the line tension contribution to the climb force.

There was no clear indication that shrinkage rate depended on distance between loops and foil surface. Loop D and E which are at different distances below the surface shrank at the same rate and loop F, which is cut by the surface but is the largest loop, had the slowest shrinkage rate as expected. However, all the loops were close to the foil surface.

Loop A, which was originially two loops that migrated together during the series, indicates that dislocation climb was very rapid when there was a nearby efficient sink for interstitials. When the two loops touched, very rapid climb took place at the resulting concave portion of the combined loop. The concave part served as an efficient sink for interstitials, be-

cause, at that point, the driving force for climb was oppositely directed or smaller than at the ends. Depending on the relative magnitude of the concave radius of curvature, the stacking fault energy and the distance to the opposite side of the loop. F_c was probably initially negative, when the two loops first joined. From observation 5 to observation 6, while the concave parts climbed outward, the outside ends of combined loop climbed rapidly inward. Therefore, these outer ends were the primary sources for the interstitials. The observations strongly suggest that the interstitial concentration in the immediate vicinity of the climbing dislocation is close to the local equilibrium value determined by F_c and that the foil surfaces are relatively poor sinks for interstitials. This later conclusion is consistent with the fact that large loop F hardly changes in size throughout the series even though it is cut by the foil surface. The foil surface may have been a poor interstitial sink because of mildly oxidizing conditions during all annealing treatments.

Figure 2 shows the shrinkage of some elongated perfect loops. They shrink from the ends where the driving force for climb is greatest due to the small radius of curvature but do not tend to adopt circular shapes, i.e. (the straight sides do not climb outward). This suggests that nucleation of jog pairs on the long straight sides requires a higher supersaturation of interstitials than that which is produced by the climb force at the ends. Jog pair nucleation on a Frank dislocation is also difficult as was shown in Fig. 1. During the oxidizing anneal (1 to 2) when the larger loops were growing all tended to develop straight sides as the existing jogs all ran out to the corners. Perfect $\frac{1}{2}$ <100> loops also showed the same rapid climb of concave segments when two loops joined. A concave segment on loop D, where nucleation of jogs was not required, was a good sink for interstitials. Loop A appears to be an exception to this behavior. This is probably

because what appears to be a concave segment in this case is actually a twist in the plane of the loop. The dipole represented by the two long sides probably changes from one of its equilibrium positions to the other. This configuration could arise from the growing together of two loops of the same burger's vector but lying on non-parallel planes.

b) Annealing Rate of Faulted Dislocation Loops:

Shrinkage rate for a number of the faulted dislocation loops at different annealing temperatures is shown in Fig. 3. For larger loops, the driving force for shrinkage is mainly due to the stacking fault, whereas for smaller loops such as H and C, line tension also plays an important role. By subtracting the contribution to shrinkage rate due to line tension, it is possible to compare loops of different sizes. Shrinkage rates that would have occurred due to the stacking fault only are shown by the dotted lines in Figure 3. Logarithmic shrinkage rates are plotted with respect to the reciprocal of the annealing temperature in Figure 4. The data gives an activation energy of 5.6 ± 0.5 ev which is consistent with that for silicon self-diffusion in this temperature range.

c) Annealing Rate of Perfect Dislocation Loops:

Elongated perfect dislocation loops such as those in Fig. 2 shrink steadily only in the length direction. This results in a constant driving force of line tension which depends on the radius of curvature at the ends of the loop. For example, the narrower loop, B, shrinks faster than loop C. However, diffusion distances cannot be assumed to be the same for these two loops.

Curve D in Fig. 5 shows the shrinkage rate of loop D and curve A shows that of loop A in Fig. 2. The shrinkage rates are constant at constant temperature. The widths of these two loops are about the same, and they show

almost the same shrinkage rates at the same temperature. The shrinkage rates for loop B and C are also shown in Fig. 5. Because of the varying loop widths and possibly also varying distance to the sink, the loop shrinkage rates are different. However, if the logarithmic shrinkage rates are plotted with respect to the reciprocal of the annealing temperatures (Fig. 4), the same activation energy for shrinkage, 5.6 ± 0.5ev, as for faulted dislocation loops is observed for all.

VI. Discussion and Conclusion

The dislocation loops formed after high temperature post implantation annealing in boron ion implanted silicon both faulted and perfect were observed to shrink in the temperature range 940°C to 1000°C. However, there existed a critical loop size above which the loop would grow instead of shrinking if any oxidation was taking place as was observed by Sanders and Dobson[19] and Prussin[16].

From the fact that two closely spaced loops (loop A in Fig. 1) migrate together during annealing and the fact that concave parts of joined loops grow outward very rapidly it is suggested that the loop shrinkage rate is controlled by the diffusion of point defects instead of by their emission rate.

For very large circular faulted dislocation loops or elongated perfect dislocation loops, the driving force for loop shrinkage depends on stacking fault energy or line tension repsectively. This driving force is essentially constant at the same temperature irrespective of the actual loop size or length. As shown by Eq. (2) or (3), the loop shrinkage rates for imperfect or perfect dislocation loops have the same temperature dependence as the silicon self-diffusion coefficient.

The activation energy for self-diffusion from radio-tracer analysis by Fairfield and Master[8] is 5.13ev. Within experimental uncertainty this is

consistent with the present results.

Because the activation energy for loop shrinkage corresponds to that for silicon self-diffusion, it is concluded that both faulted Frank dislocation loops and perfect loops, remaining after the linear boron precipitates have been redissolved are composed mostly of silicon atoms.

VII. Acknowledgement

This work was done under the auspices of the Materials and Molecular Research Division, Lawrence Berkeley Laboratory, of the U.S. Energy Research and Development Administration.

Reference

1. J. Silcox and M.J. Whelan, Phil. Mag. 5, 1, (1960).
2. J. M. Edington and R. E. Smallman, Phil. Mag. 11, 1109, (1965).
3. J. P. Tartour and J. Washburn, Phil. Mag., 8, 1257, (1968).
4. J. Washburn and M. J. Yokota, Cryst. Lattice Defects, 1, 23, (1969).
5. V. C. Kannan and G. Thomas, J. Appl. Phys., 37, 2369 (1966).
6. J. Narayan and J. Washburn, Phil. Mag. 26, 1179, (1972).
7. J. Narayan and J. Washburn, Cryst. Lattice Defects, 3, 91, (1972).
8. J. M. Fairfield and B. J. Masters, J. Appl. Phys., 38, 3148, (1967).
9. W. Wu, L. J. Chen, J. Washburn and G. Thomas, J. Appl. Phys. 45, 563, (1974).
10. D. N. Seidman and R. W. Bolluffi, Phil. Mag. 13, 649, (1966).
11. M. J. Whelan, Phil. Mag. 14, 195 (1966).
12. P. S. Dobson, P. J. Goodhew and R. E. Smallman, Phil. Mag. 16, 9, (1967).
13. R. N. Ghoshtagore, Phys. Rev. Letters 25, 866 (1970).
14. P. S. Dobson, Phil. Mag. 26, 567, (1971).
15. P. S. Dobson, Phil. Mag. 26, 1301, (1972).
16. S. Prussin, J. Appl. Phys, 45, 1635, (1974).
17. A. Seeger, Rad. Effects, 9, 15, (1971).
18. D. J. Bacon and A. G. Crocker, Phil. Mag. 12, 195, (1966).
19. I. R. Sanders and P. S. Dobson, Phil. Mag. 20, 881 (1969).

Figure Captions

Fig. 1 Sequences showing the shrinkage of Frank dislocation loops. (1) to (4) were taken after annealing at 942°C for one hour respectively. (5) to (7) were taken after annealing at 970°C for 15, 15, and 30 minutes respectively. (8) and (9) were taken after annealing at 1001°C for 10 and 20 minutes respectively.

Fig. 2 Sequence showing the shrinkage of perfect dislocation loops. Same heat treatment as in Fig. 1.

Fig. 3 Loop sizes of Frank dislocation loops vs. annealing time at three different temperatures.

Fig. 4 Loop shrinkage rates vs. reciprocal of annealing temperature.

Fig. 5 Loop lengths of perfect elongated dislocation loops vs. annealing time at three different temperatures.

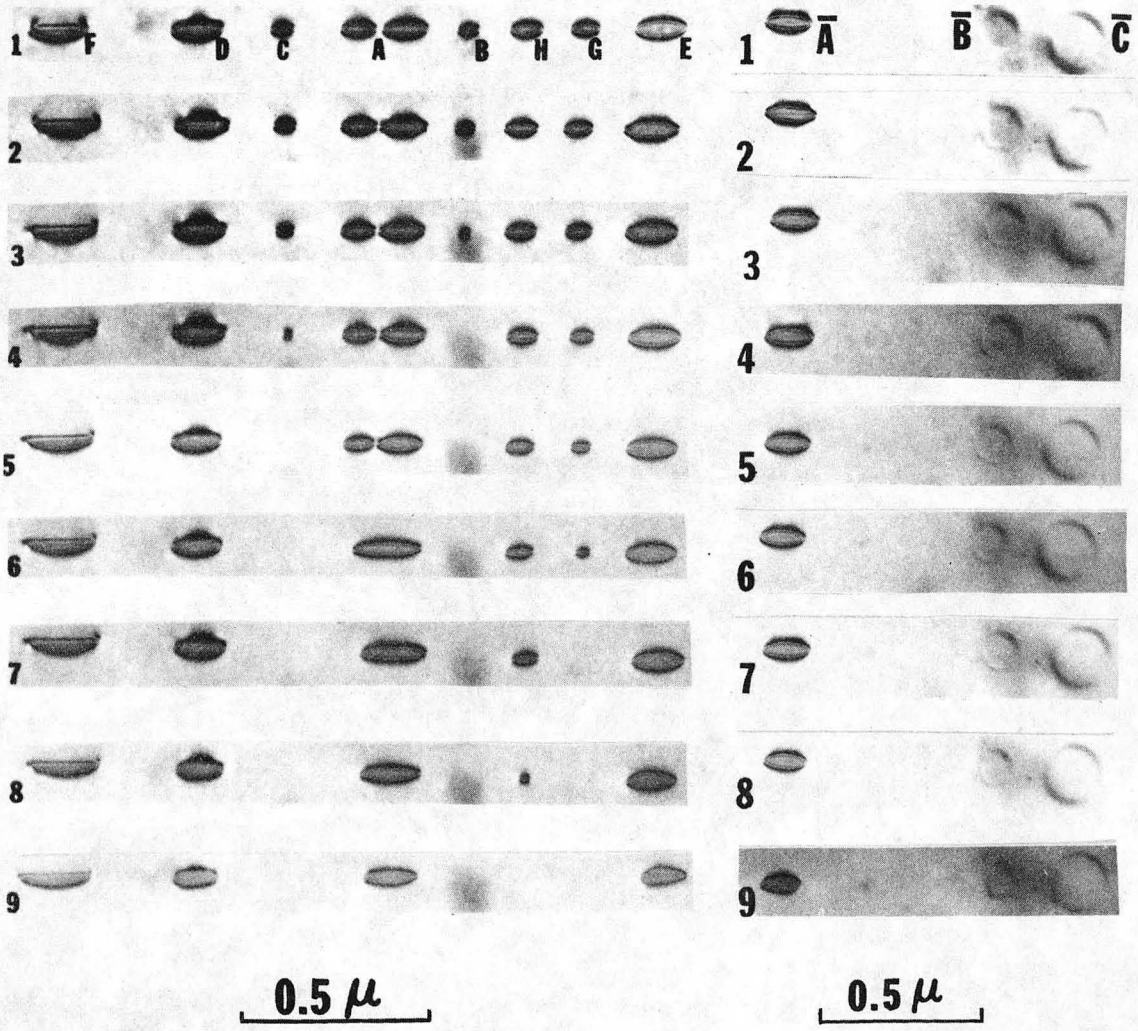

XBB-760-10015

FIG. 1

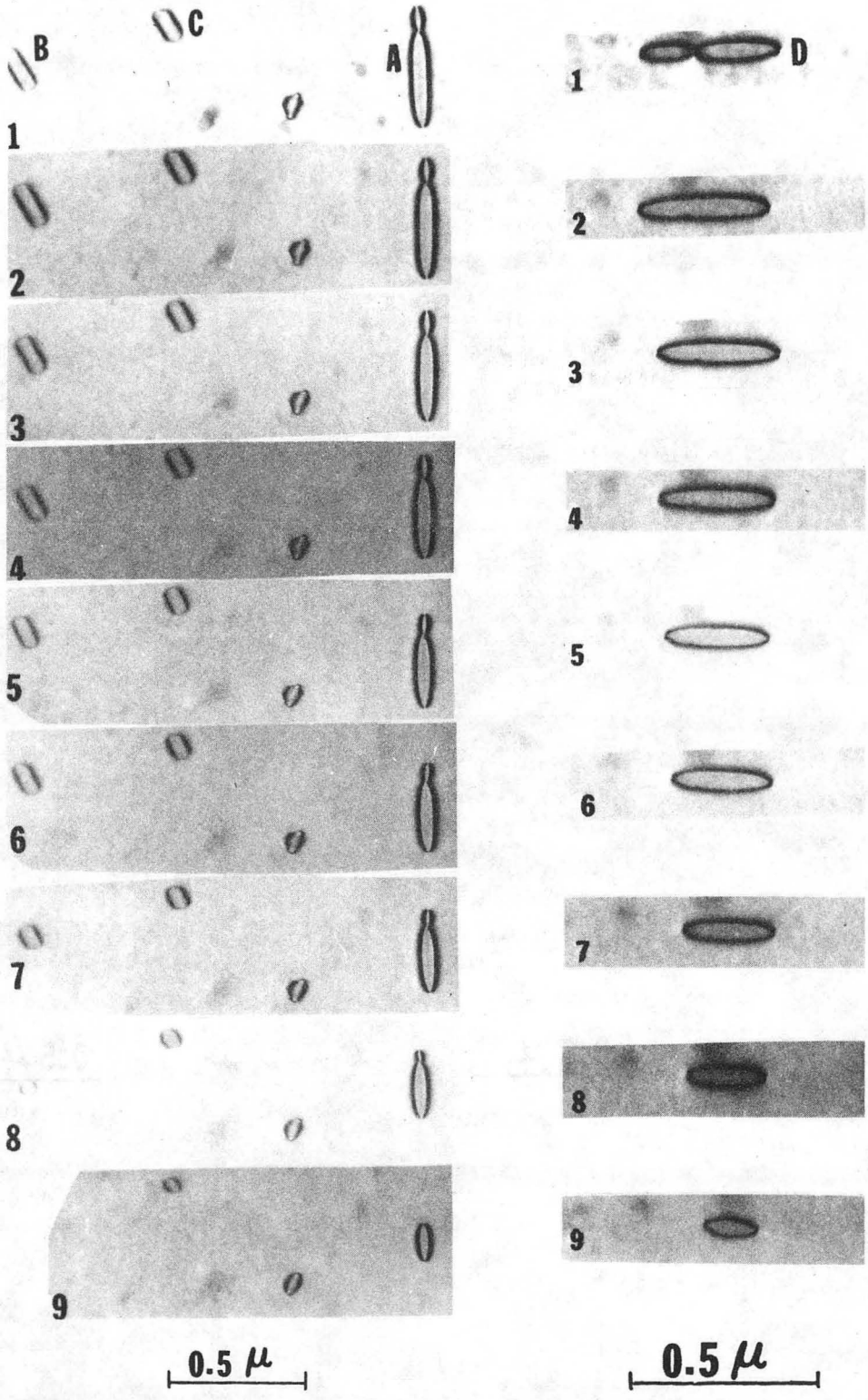

XBB-760-10014

FIG. 2

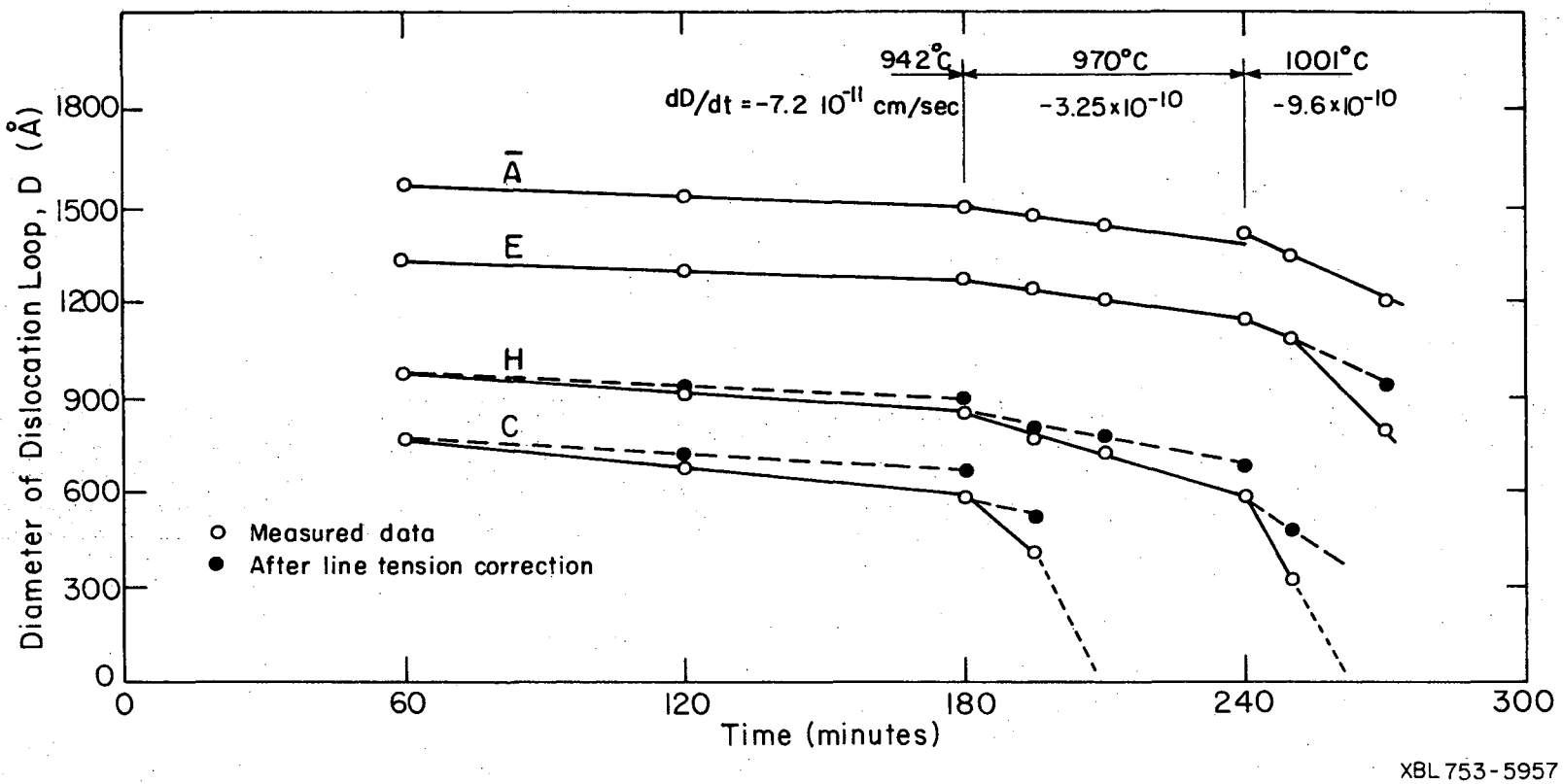

FIG. 3

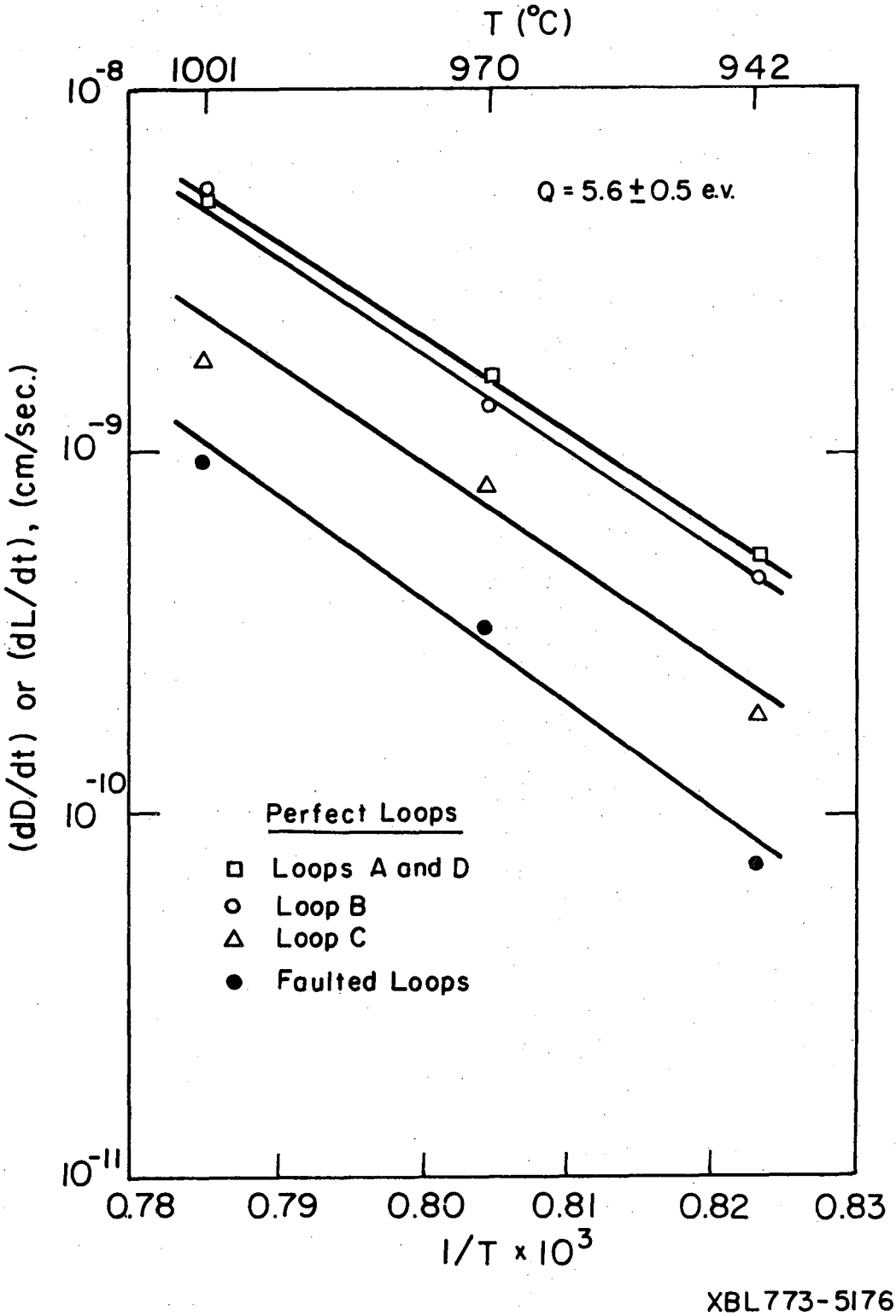
T (°C)
1001
970
942
10^{-8}
10^{-9}
10^{-10}
10^{-11}
Q = 5.6 ± 0.5 e.v.
(dD/dt) or (dL/dt), (cm/sec.)
Perfect Loops
Loops A and D
Loop B
Loop C
Faulted Loops
0.78
0.79
0.80
0.81
0.82
0.83
$1/T \times 10^3$
XBL773-5176

FIG. 4

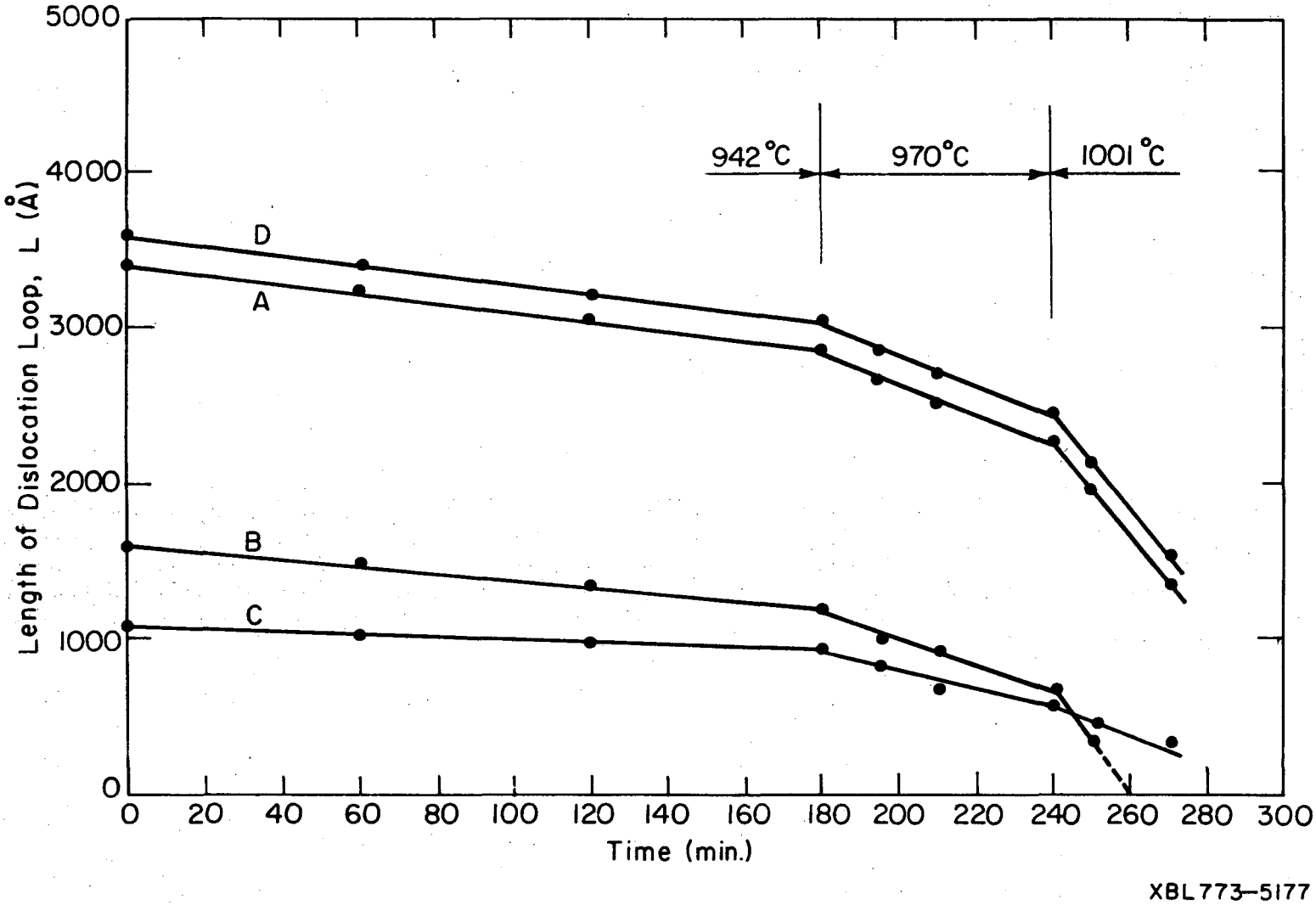

FIG. 5

TECHNICAL INFORMATION DIVISION
LAWRENCE BERKELEY LABORATORY
UNIVERSITY OF CALIFORNIA
BERKELEY, CALIFORNIA 94720